Title

Pangenome of U.S. ex-PVP and Wild Sorghum Reveals Structural Variants and Selective Sweeps Shaping Adaptation and Trait Improvement

Running Title

Pangenome of U.S. ex-PVP and Wild Sorghum

Authors

Justine K. Kitony [1], Emily Murray [1], Kelly Colt [1], Ryan Lynch [1], Nick Allsing [1], Nolan T. Hartwick [1], Tiffany Duong [1], Jocelyn Saxton [2], Nadia Shakoor [2], Todd P. Michael [1,3]

Affiliation

1. Plant Molecular and Cellular Biology Laboratory, Salk Institute for Biological Studies, La Jolla, CA, USA
2. Donald Danforth Plant Science Center, Olivette, MO, USA
3. Science and Conservation, San Diego Botanical Garden, Encinitas, CA, USA

Corresponding Author

Todd P. Michael, toddpmichael@gmail.com, tmichael@salk.edu

Key Words

Expired Plant Variety Protection (ex-PVP), sorghum pangenome, selective sweep, structural variants (SVs), long-read sequencing, chromosome- level assemblies, presence–absence variation (PAVs), and copy number variation (CNVs)

Abstract

Sorghum is a cereal crop grown for food, feed, and biofuel, yet the genomic diversity of elite commercial lines remains underexplored. Here, we assembled a sorghum pangenome from long-read sequences of 46 U.S. ex-Plant Variety Protection Act (ex-PVP) cultivars and a haplotype-resolved assembly of one wild accession. The pangenome revealed largely conserved genomic architecture across elite lines but identified presence–absence variations (PAVs) in 28% of gene families, including genes involved in stress responses and starch metabolism, such as *STARCH BRANCHING ENZYME I (SBE1)*. Selective sweep analyses detected strong signals at key flowering-time loci (*Ma1/SbPRR37, Ma2, Ma6*) and circadian/light regulators (*PHOT1, DET1, XAP5*), with *PHYA* showing copy number variations (CNVs). Analysis of 24 wild accessions, beyond the core pangenome panel, detected CNVs in *MULTIDRUG AND TOXIC COMPOUND EXTRUSION (MATE)* transporters, potentially reflecting selection or breeding for enhanced herbicide detoxification. These results highlight breeding-shaped regions and position the pangenome as a resource for sorghum improvement.

Main

Sorghum (*Sorghum bicolor*) is a C_4 monocot renowned for its exceptional resilience to drought, heat, and low-fertility soils [1]. As the fifth most important cereal crop globally, it is cultivated for diverse purposes—including food, animal feed, alcoholic beverages, and biofuel—driven by its nutritional value (high protein, essential micronutrients, gluten-free) and adaptability to abiotic stresses. These attributes make sorghum a vital crop for enhancing food security and promoting sustainable agriculture in the face of climate change [1–5].

Sorghum, originating in Africa, was introduced to the U.S. in the late 19th century through germplasm collections of sweet, grain, and sudangrass types [6–9]. Early public breeding programs played a key role in improvement, with notable successes such as the development of the drought-tolerant 'Atlas' variety in 1936 [8]. The discovery of cytoplasmic male sterility (CMS) and corresponding fertility restorer (Rf) genes in the mid-20th century enabled commercial hybrid production, boosting yields by up to 40% by the 1950s [7,10].

From the 1960s to 1980s, U.S. sorghum breeding shifted toward the private sector. Companies like Pioneer Hi-Bred began developing proprietary hybrids protected for 20 years under the 1970 Plant Variety Protection Act (PVPA). These hybrids featured dwarf stature (suitable for mechanical harvesting), early maturity, stay-green traits (e.g., SC35), and resistance to anthracnose, greenbug, downy mildew, and smut [7,11]. As a result, the United States emerged as the world's leading exporter of sorghum, accounting for approximately 15% of global production [12–14].

Most genomic studies in sorghum have relied on the 'BTx623' reference genome [1,15,16], which represents a single grain-type line and fails to capture the full extent of genetic variation within cultivated germplasm. This reference bias limits the discovery of presence–absence variations (PAVs), SVs, and CNVs that underlie important agronomic traits [17–19]. Pangenome approaches provide a broader framework for characterizing SVs across diverse accessions [20,21]. Short-read-based pangenomes in sorghum have identified 35,719 genes, with ~53% showing PAVs and 79 loci absent from the reference genome [22,23]. Long-read-based pangenomes have uncovered even greater diversity—44,079 gene families across 16 accessions, including 222.6 Mb of novel sequence [21]. Similarly, high-quality assemblies from ten bioenergy sorghum genotypes uncovered thousands of SVs, including those associated with traits like iron transport [24]. Accessibility of long-read sequencing (e.g., PacBio HiFi, ONT) is now enabling detection of novel gene content and SVs associated with traits [25,26].

From early domestication to modern crop improvement, selection—both natural and artificial—has left footprints across plant genomes. These genomic signatures reveal how crops have been shaped for key agronomic traits across time and environments. In wheat, genomic scans have uncovered loci controlling flowering time [27]; in rice, genes conferring pathogen resistance [28]; and in maize and cotton, variants linked to yield and stress tolerance [29,30]. Sorghum is no exception. Selective sweeps have been reported at loci such as *SHATTERING1 (SH1)*, which affects seed dispersal, and the *DRY NAC* transcription factor, involved in sugar accumulation [31–33]. Beyond selection on classical domestication and yield-related genes, natural and artificial selection has also acted on sorghum's internal time-of-day (TOD) regulatory network (circadian rhythms), which governs key developmental processes such as vegetative growth and reproductive timing [34–36]. These rhythms also influence the optimal timing of agricultural inputs

92 and support sorghum's adaptation across broad latitudinal ranges. Selection at the *Ma1* locus,
93 encoding *PSEUDO-RESPONSE REGULATOR 37 (SbPRR37)*, exemplifies adaptation to
94 temperate climates and remains a target in modern breeding for bioenergy [37]. Yet many regions
95 under selection remain unresolved due to the underrepresentation of elite commercial
96 germplasm genomes and the complexity of sorghum's breeding history [38–40].
97
98 Here we present a long-read-based sorghum pangenome constructed from 46 U.S. ex-PVP
99 lines and wild accessions, revealing approximately 28% PAVs in gene families, localized SVs,
100 selection signatures in TOD loci, and CNVs associated with key agronomic traits. This resource
101 enhances our understanding of sorghum adaptation and provides a foundation for genomic
102 characterization and crop improvement through modern breeding approaches [39,41,42].
103
104 **Results**
105 ***High-Quality Genome Assemblies of Ex-PVP and Wild Sorghum Accessions***
106 We assembled high-quality genomes for 46 elite ex-PVP lines and both haplotypes of a wild
107 sorghum accession, 'PI156549.' Genome sizes ranged from 610 to 779 megabases (Mb), with
108 confirmed gene models ranging from 30,000 to 33,000 per genome (Fig. 1a). The new
109 assemblies achieved levels of contiguity comparable to the 'BTx623' reference [16], with N50
110 values reaching up to 19 Mb (Fig. 1b, Supplementary Fig. 1a-c, Supplementary Table 1),
111 reflecting reference-quality assemblies across the dataset.

112 Assembly quality was assessed using the LTR Assembly Index (LAI), with scores ranging from
113 20 to 30, consistent with reference-grade assemblies (Fig. 1c, Supplementary Table 1). BUSCO
114 analysis confirmed high completeness of both genome assemblies (92.60–99.10% complete
115 BUSCOs) and predicted proteins (91.70–98.50%), supporting an accurate gene space view
116 across diverse genotypes (Supplementary Table 2).

117 Total interspersed repeat content showed a strong correlation with genome size ($R^2 = 0.834$;
118 Fig. 1d), underscoring the dominant role of repeats in genome expansion. Centromeric tandem
119 repeat expansions also correlated with genome size ($R^2 = 0.747$; Supplementary Fig. 1d).
120 Transposable elements (TEs), which make up ~65% of each genome assembly (Fig. 1e),
121 dominate sorghum genome composition and have broadly shaped its structure, regulation, and
122 adaptability [43]. Among these, retroelements (LTRs) were the most abundant class, followed by
123 DNA transposons and rolling-circle elements. Notably, a substantial proportion (~15–20%) of
124 the TEs content remained unclassified across genomes, even when using high-resolution
125 annotations from Helixer [44]. This unclassified fraction highlights the presence of highly divergent
126 or lineage-specific elements that escape conventional TEs classification approaches [45,46].

127 Analysis based on K-mer profiles revealed genetic clustering among the ex-PVP lines, with
128 some accessions showing closer relatedness but overall forming a cohesive group. The wild
129 accession formed a distinct outgroup (Fig. 1f), consistent with its contribution to novel K-mers in
130 the PanKmer collector's curve, which shows an open pangenome (Supplementary Fig. 1e,
131 Supplementary Table 3).

132

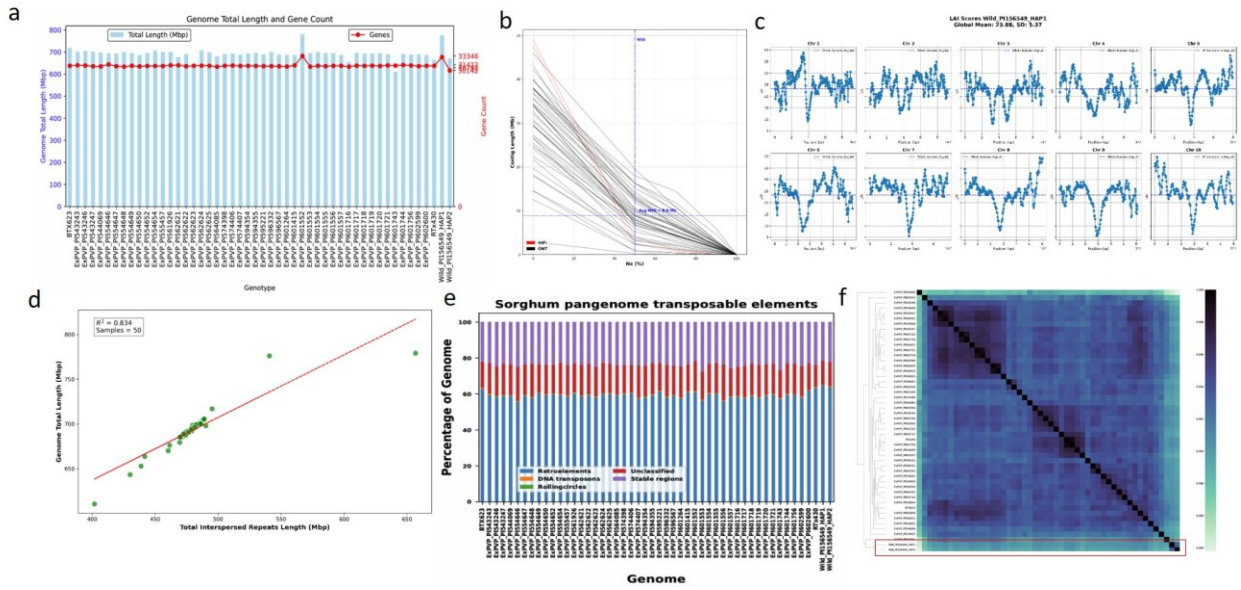

Fig. 1: Genome Assembly Metrics, Transposable Elements (TEs), and Genome Architecture of the U.S. Ex-PVP and Wild Sorghum Pangenome.
a, Genome length (Mb; right y-axis) and gene count (left y-axis) across assembled accessions. **b**, Assembly contiguity measured by N50 values (Mb). **c**, Example LTR Assembly Index (LAI) distribution across chromosomes for the wild accession 'PI156549' Haplotype 1, with a global mean of 23.88 and a standard deviation (SD) of 5.37. **d**, Correlation between total interspersed repeat content and genome size. **e**, TEs classes expressed as a percentage of genome size. Colors represent TEs categories as shown in the legend. **f**, Clustered heatmap of adjacency values based on pairwise K-mer comparisons between genomes. The ex-PVP lines exhibit largely conserved nucleotide identity, forming a homogeneous cluster distinct from the wild accession haplotypes (red box). Pangenome accessions include elite ex-PVP lines and wild sorghum samples. Full sample and sequencing details are in Supplementary Table 1; source data are available in the associated data file.

Sorghum Pangenome Captures Gene Diversity Missed by the BTx623 Reference

Using the constructed pangenome, we characterized gene content variation that would be overlooked when relying solely on the 'BTx623' reference[16]. In total, 36,004 gene families (orthogroups) were identified (Supplementary Table 4), comprising 71.5% core genes, 2.2% soft-core genes, 16.7% dispensable genes, and 9.6% private genes (Fig. 2a). Gene accumulation curves showed continued pangenome growth and core genome decline, approaching a plateau that suggests most gene diversity was captured (Fig. 2b). A power law fit of novel gene family discovery ($a = 4.13$, $R^2 = 0.999$) confirmed a highly closed sorghum pangenome (Fig.2c) [47]. Comparison to the 'BTx623' reference revealed 6,389 additional gene families, many absent from the reference but present in wild and elite ex-PVP lines (Fig. 2d). Gene PAVs analysis across the 50 genomes revealed shared gene family patterns among the ex-PVPs (Fig. 2e), with genespace visualization further highlighting overall gene conservation across chromosomal segments (Fig. 2f).

The 6,389 pangenome exclusive orthogroups (Fig. 2d) include key KEGG functions absent from the reference 'BTx623' (Fig. 2g), such as chloroplast electron transport components—ATP SYNTHASE SUBUNIT BETA (ATPB), NADH DEHYDROGENASE SUBUNIT H (NDHH), and NADH DEHYDROGENASE SUBUNIT F (NDHF); stress response regulators—GLUTATHIONE S-TRANSFERASE TAU 1 (GSTU1) and ABSCISIC ALDEHYDE OXIDASE 3 (AAO3); and specialized metabolism genes—FLAVONOID 3'-HYDROXYLASE (F3'H), SALICYLIC ACID CARBOXYL METHYLTRANSFERASE (SAMT) and TREHALOSE-6-PHOSPHATE SYNTHASE 1 (TPS1). Notably detected is STARCH BRANCHING ENZYME I (SBE1), which controls starch branching and may harbor allelic variants preferentially retained in ex-PVP lines for improved grain quality or digestibility traits [48]. In total, 982 KEGG orthology (KOs) associations were identified across these orthogroups (Supplementary Table 5). These KOs suggest hidden variation in energy metabolism, detoxification, and hormone-mediated stress adaptation, echoing findings in other crops where pangenome analyses revealed adaptive traits beyond reference genomes [49]. These findings also demonstrate the value of the pangenome in uncovering agronomically relevant diversity that is missed by single-reference approaches [50].

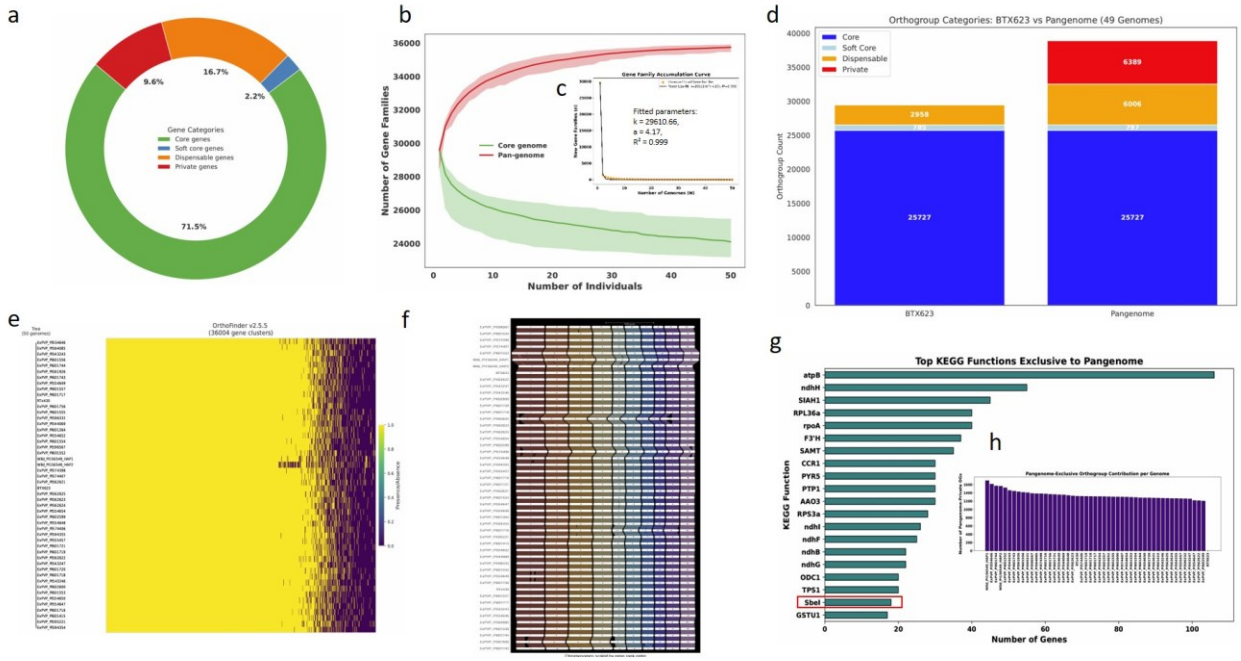

Fig. 2: Pangenome-Wide Gene Presence–Absence Variation Reveals Genes Missing from the BTx623 Reference.

a, Classification of 36,004 gene families into core (green), soft-core (blue), dispensable (orange), and private (red). **b,** Collectors curves showing pan- and core-genome orthogroups dynamics across genomes sampled. **c,** Power law fit of novel gene family discovery indicating a closed sorghum pangenome as evidenced by the plateauing collectors curve **d,** Stacked bar plot comparing gene categories in the 'BTx623' reference (left) and the full pangenome (right), the red bar reveals 6,389 additional gene families present in the pangenome. **e,** Gene family presence–absence variation across accessions highlights shared patterns among ex-PVP lines. Yellow indicates presence; black indicates absence. **f,** Genespace riparian plot illustrating

macro-synteny across sorghum genomes, revealing broad genic similarity and a mostly conserved structure with a few notable rearrangements. **g,** a bar plot of enriched KEGG orthology (for genes in pangenome-exclusive orthogroups). The orthologies include ATP synthase subunit beta (atpB), NADH dehydrogenase subunits (ndhH, ndhI, ndhF, ndhB, ndhG), E3 ubiquitin-protein ligase SIAH1 (SIAH1), ribosomal protein L36a (RPL36a), DNA-directed RNA polymerase subunit alpha (rpoA), Flavonoid 3'-hydroxylase (F3'H), Salicylic acid carboxyl methyltransferase (SAMT), Cinnamoyl-CoA reductase 1 (CCR1), Pyrimidine 5'-nucleotidase (PYR5), Protein tyrosine phosphatase 1 (PTP1), Abscisic aldehyde oxidase 3 (AAO3), ribosomal protein S3a (RPS3a), Ornithine decarboxylase 1 (ODC1), Trehalose-6-phosphate synthase 1 (TPS1), Starch branching enzyme I (SBEI), and Glutathione S-transferase tau 1 (GSTU1), suggesting functional convergence in stress response, metabolism, and development. The SBEI gene, which plays a role in starch metabolism and grain quality, is highlighted in red. **h**, A bar plot showing how much each genome contributes to the pangenome-exclusive orthogroups. Source data are provided in the Source Data file.

Structural Variants Underpin Genomic Diversity and Adaptive Traits in Elite ex-PVP Sorghum Lines

A total of 1,118,641 SVs were identified across the pangenome, including insertions, deletions, duplications, inversions, and translocations (Fig. 3a), with the highest individual SVs (42,096) found in wild haplotype 1 (Supplementary Table 6). Insertions and deletions had median sizes of 319 bp and 346 bp, respectively, reflecting a predominance of short to medium-sized INDELs with potential regulatory or coding impacts (Fig. 3b). SVs also overlapped promoter and exon regions, with mean lengths of 1,744 bp and 2,000 bp, respectively (Fig. 3c), suggesting functional consequences for gene expression and/or protein activity. Macro-synteny analysis revealed broadly conserved chromosomal architecture with lineage-specific large-scale rearrangements, including a ~5 Mb inversion on chromosome 5 annotated to a wall-associated kinase (WAK) gene associated with cold tolerance (Fig. 3d). Pairwise comparisons across the pangenome highlighted extensive SV-based divergence, particularly between wild and elite ex-PVP accessions (Fig. 3e, Supplementary Table 7). SVs were unevenly distributed across the genome, with higher densities in pericentromeric and telomeric regions, consistent with suppressed recombination and TE accumulation (Fig. 3f) [51].

Among key SVs, a 105 bp deletion was detected in *Sobic.001G445700.v5.1*, a gene homologous to *Arabidopsis thaliana β-1,3-GLUCANASE A6* gene. The deletion removes a conserved glycosidase domain (Fig. 3g), likely impairing its role in cell wall remodeling and defense. The variant is predominantly present in elite ex-PVP lines and absent in wild accessions, which retain the full gene (Fig. 3h), suggesting this deletion may reflect relaxed defense investment under high-input agricultural systems (e.g., pesticide applications). This pattern could result from reduced pathogen pressure in managed environments or represent a trade-off favoring growth and yield over defense. Whole-genome alignments further confirmed genotype-specific loss of functional sequence, as evidenced by the absence of mapped reads in lines carrying the deletion (Fig. 3i). These findings highlight SVs as a distinct and functionally relevant layer of genomic variation contributing to cultivated sorghum diversity and productivity.

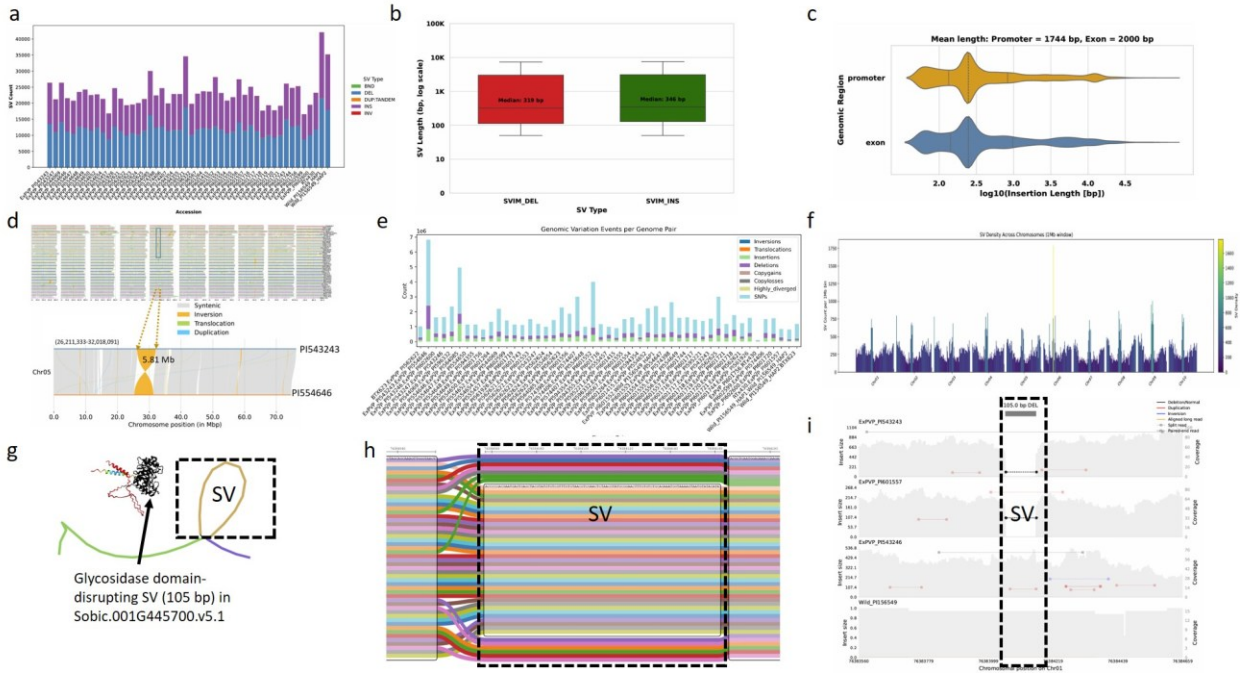

Fig. 3: Structural Variants in the Sorghum Pangenome Impact Gene Function and Stress-Related Pathways.

a, Total number of structural variants (SVs) identified across the 50-genome pangenome; wild haplotype 1 exhibited the highest SV count (42,096), highlighting elevated genomic diversity. **b**, Length distribution of insertions and deletions (INDELs), highlighting the prevalence of short to medium-sized variants. **c**, Distribution of SVs lengths within promoter and exon regions, with potential impacts on gene regulation and coding sequences. **d**, Macro-synteny karyotype plot illustrating conserved chromosomal structure and large-scale rearrangements across sorghum genomes, including a ~5 Mb inversion on chromosome 5 linked to a wall-associated kinase (WAK) candidate gene associated with cold tolerance. **e**, Distribution of pairwise genomic differences across the pangenome, illustrating inter-accession genomic diversity. **f**, Genome-wide SVs density along sorghum chromosomes, with enriched regions corresponding to pericentromeric and telomeric zones. **g**, Pangenome graph and 3D structural visualization of the *Sobic.001G445700.v5.1* protein, a homolog of the *Arabidopsis thaliana β-1,3-GLUCANASE A6* gene involved in plant defense and cell wall remodeling. A 105 bp deletion in this gene disrupts the conserved glycosidase domain (black), likely impairing enzymatic function and suggesting a potential breeding signature for reduced defense investment under high-input agricultural systems. **h**, Presence-absence pattern of the *Sobic.001G445700.v5.1* SVs across the pangenome, distinguishing elite lines from wild accessions. **i**, In silico validation of the structural variant, based on whole-genome read alignments viewed in IGV, confirmed genotype-specific

258 loss of functional sequence—observed in accessions with the 105 bp deletion
259 (ExPVP_PI543243, ExPVP_PI601557) compared to those without (ExPVP_PI543246,
260 Wild_PI565549). Source data are provided in the Source Data file.
261
262 ***Selection Targets Circadian and Photoperiod Genes in U.S. Sorghum***
263 We aligned the whole genome sequences of 46 ex-PVP and 25 wild sorghum accessions
264 (Supplementary Table 1) to the 'BTx623' reference genome. SNPs were called across all
265 accessions, and after quality filtering, 34,035 high-confidence biallelic SNPs were retained for
266 population structure analysis. Using this dataset, ADMIXTURE analysis (K = 1–10) identified K
267 = 2 as the optimal number of ancestral populations based on the lowest cross-validation error
268 (Supplementary Fig. 2a-b). PCA on the same SNP dataset further detected three genetic
269 clusters, separating ex-PVP lines from two distinct wild subgroups (wild1 and wild2;
270 Supplementary Fig. 2c-f). Based on this population structure, we performed genome-wide
271 selection scans using FST, XP-CLR, and π-ratio to identify genomic regions under differential
272 selection between wild and cultivated accessions.

273 Selective sweep analysis revealed that XP-CLR and π-ratio identified the most candidates,
274 while overlapping regions from all three methods defined smaller, high-confidence gene sets
275 under strong selection (Supplementary Tables 8-9). Multiple sweep regions differentiated wild
276 and elite ex-PVP lines (Fig. 4a, Supplementary Fig. 3b-d), with strong signals co-localizing with
277 known domestication genes involved in auxin transport, seed dormancy, and aromatic amino
278 acid biosynthesis (Fig. 4b). These pathways are critical for traits such as plant architecture,
279 seed dispersal, and germination.

280 Although a *β-1,3-GLUCANASE* showed structural disruption in ex-PVP lines (Fig. 3g-i),
281 genome-wide sweeps reveal positive selection on other immune-related pathways, such as
282 *PATTERN RECOGNITION RECEPTOR (PRRs)* signaling and innate immune activation,
283 suggesting a shift in defense strategy rather than an overall reduction. Enriched GO terms also
284 indicate that modern breeding emphasized immune signaling, xenobiotic transport,
285 phospholipase activity, and RNA export (Fig. 4b)—reflecting a broader focus on stress
286 resilience and metabolic efficiency under high-input agricultural systems.

287

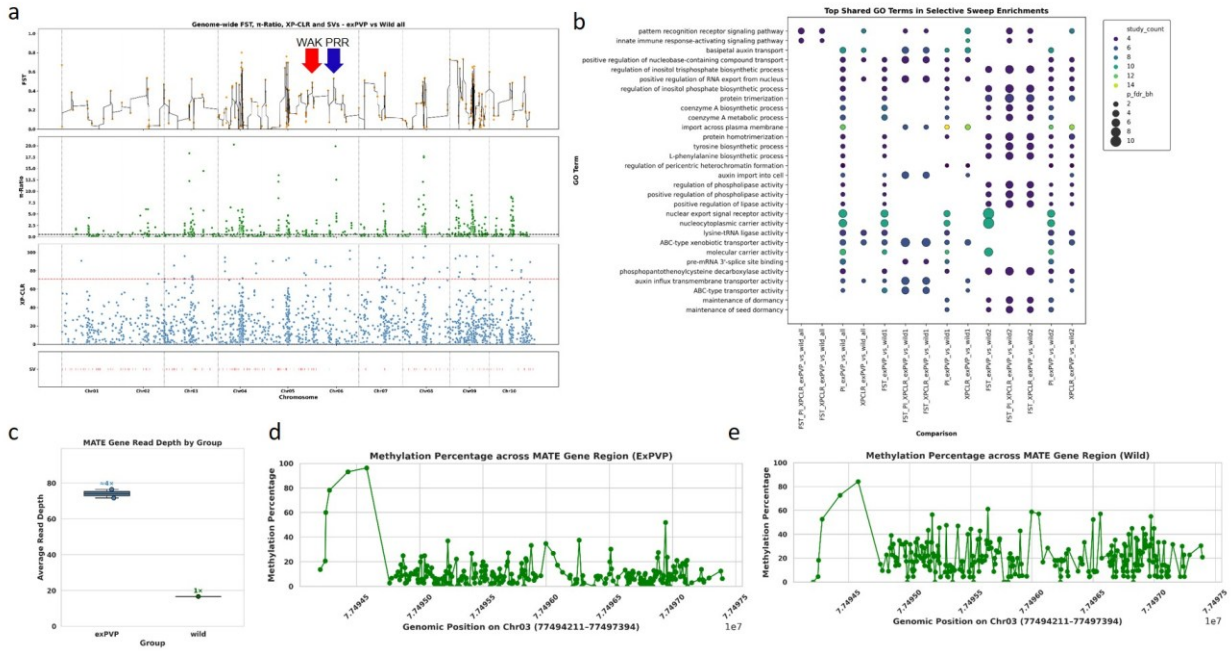

Fig. 4: Selection Signatures During Sorghum Improvement Reveal Functional Divergence and Adaptive Loci.
a, Genome-wide selective sweep signals (FST, π, XP-CLR) across chromosomes comparing 25 wild vs. 46 ex-PVP accessions. The bottom track shows large structural variants identified across the chromosomes. The red arrow marks the position of a *WALL-ASSOCIATED RECEPTOR KINASE* gene *(Sobic.005G179200*) on chromosome 5 (~71 Mb), a member of a gene family known to regulate cell wall integrity and stress signaling under cold conditions. The blue arrow indicates the *PSEUDO-RESPONSE REGULATOR 37* gene (*SbPRR37*, *Sobic.006G057866*) on chromosome 6 (~41 Mb), a key regulator of photoperiod sensitivity and flowering time in sorghum. **b**, Gene Ontology (GO) enrichment of genes within top 5% sweep regions, highlighting domestication and improvement functions (e.g., auxin transport, immune signaling, dormancy) from various population comparisons and methods shown on the x-axis. **c**, Copy number variation of the *MULTIDRUG AND TOXIC COMPOUND EXTRUSION (MATE*) gene between representative wild and ex-PVP lines, showing approximately fourfold higher copy number in the ex-PVP lines. **d**, methylation percentage across *MATE* gene loci in ex-PVP, indicating low levels across the gene body region. **e**, methylation percentage across *MATE* loci in wild accession showing dynamic levels across the gene body region. Both accessions exhibit higher methylation levels in the promoter region. Source data are provided in the Source Data file.

Enrichment analysis of genes under selection highlighted key regulators of circadian rhythm and flowering time, including *PRR7* and *PRR95*, and *PRR95*, core components of the circadian clock, as well as *CO* and *PHOT1*, which mediate photoperiodic flowering (Supplementary Table 10). Genes involved in seasonal development—such as *FRIGIDA (FRI)*, *VRN2B,* and *VRN3B*—were also enriched, suggesting coordinated selection on flowering pathways. Additional targets included *REGULATORY-ASSOCIATED PROTEIN OF TOR 1A (RAPTORA)*, *TARGET OF*

RAPAMYCIN (TOR), *GRAIN NUMBER, PLANT HEIGHT, AND HEADING DATE 7 / MATURITY 6 (GHD7/MA6)*, and *XAP5 CIRCADIAN TIMEKEEPER (XCT)*, implicating broader roles for metabolic and growth regulation in adaptation [52]. These loci lie within sweep regions analogous to those reported in other crops—for example, selection on *DRIVERS OF THE CIRCADIAN CLOCK (DOC)* in barley has been shown to modulate rhythmicity and reproductive traits under domestication [53]. The co-selection of these interconnected regulators underscores a multifaceted strategy favoring clock-modulated traits, offering breeders a powerful entry point to fine-tune flowering time, growth rate, and environmental responsiveness in modern sorghum improvement programs.

Further analysis of genomic regions associated with flowering time, photoperiod sensitivity, and circadian regulation revealed a strong signal at the *SbPRR37 locus (Sobic.006G057866)*, the classical *MATURITY 1 (Ma1)* gene in sorghum. Its closest *Arabidopsis thaliana* ortholog is *PRR7* (Fig. 5a, Supplementary Table 11). We detected CNVs at *SbPRR37*, with two copies present in most cultivated genotypes but only one in wild haplotype 2, suggesting reduced redundancy or differential selection pressure in wild populations. Additional sweep intervals contained other circadian and flowering regulators, including *PRR7* (Sobic.001G411400), PRR95 (*Sobic.002G275100*), *Ma2* (*Sobic.002G302700*), and *GDH7/Ma6* (*Sobic.006G004400*), supporting the hypothesis that multiple maturity genes (*Ma1–Ma6*) have been targets of selection during domestication and improvement [37].

Several other sweep regions harbored genes involved in florigen signaling and circadian entrainment, such as *VERNALIZATION 3B (VRN3B, Sobic.003G173032*), *CONSTANS (CO, Sobic.010G115800*), and *PHOTOTROPIN 1 (PHOT1, Sobic.008G001000*). Selection signals also overlapped with key metabolic and photomorphogenic regulators, including *TARGET OF RAPAMYCIN (TOR)* (Sobic.009G109200), *REGULATORY-ASSOCIATED PROTEIN OF TOR 1A (*RAPTORa) (Sobic.005G008800), *XAP5 CIRCADIAN TIMEKEEPER (XCT)* (Sobic.002G277600), and *DE-ETIOLATED 1 (DET1)* (Sobic.007G058100). Structural variation, including PAVs and CNVs, was also evident at the *PHYTOCHROME A (PHYA)* and *FLOWERING LOCUS T (*FT), alongside enrichment of core circadian components. Notably, regulators such as *CIRCADIAN CLOCK ASSOCIATED 1 (CCA1)* appeared to be dicot-specific—present in *Arabidopsis thaliana* and *Brassica napus* but absent from the sorghum genome (Fig. 5).

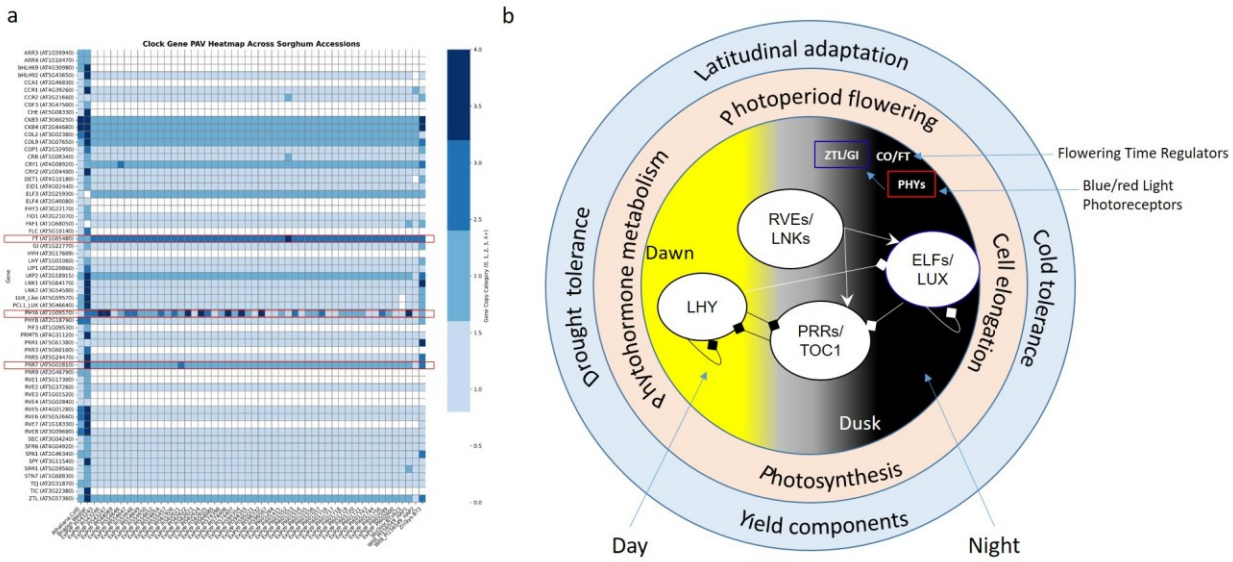

Figure 5. Time-of-Day (TOD) Gene Variation and Model of the Sorghum Circadian Clock Network.
a, Variation in circadian clock and flowering-time genes reveals distinct selection pressures in cultivated sorghum. Copy number expansion of the circadian photoreceptor PHYTOCHROME A (PHYA) and the clock regulator PSEUDO-RESPONSE REGULATOR 37 (SbPRR37, Sobic.006G057866)—orthologous to PRR7 (AT5G02810) and PRR3 (AT5G60100) in Arabidopsis thaliana—reflects selection on the circadian system, while duplication of the florigen gene FLOWERING LOCUS T (FT) indicates selection on flowering-time pathways. PHYA and FT are highlighted in red boxes. These patterns suggest targeted adaptation to seasonal and latitudinal environments via independent tuning of clock and flowering components. **b**, Schematic representation of interlocked transcriptional feedback loops that drive circadian rhythms, allowing coordination with environmental signals such as light and temperature. The central area illustrates core clock regulatory interactions, adapted from Bendix et al. (2015) [37]. Yellow and black regions represent day and night, respectively. Arrows with pointed ends indicate activation; diamond-tipped arrows indicate repression. The orange-shaded middle layer denotes signaling and physiological pathways directly regulated by the circadian clock, while the outer blue-shaded ring highlights traits influenced by clock-controlled outputs. See supplementary notes for details. Source data are provided in the Source Data file.

Copy Number Expansion and Differential Methylation of the MATE gene in ExPVP lines
CNVs analysis based on read depth revealed four copies of the *MATE* (*Sobic.003G403000.v5.1*) gene in ex-PVP lines compared to a single copy in the wild accession (Fig. 4c). This copy number expansion coincides with a marked reduction in DNA methylation across the gene body in the ex-PVP lines, whereas the wild accession exhibited higher and more variable methylation across the same region (Fig. 4d). The lower methylation in ex-PVP accessions, particularly within the gene body (Supplementary Fig. 4), suggests epigenetic reprogramming likely associated with transcriptional activation of duplicated *MATE* copies. In contrast, the higher and fluctuating methylation levels in the wild accession may reflect transcriptional repression or tighter regulation (Fig. 4e). These patterns are consistent with

selective amplification and epigenetic remodeling of *MATE* in elite germplasm to support traits such as xenobiotic transport or abiotic stress response [54].

Discussion

This study explores SVs, gene PAVs, and epigenomic remodeling in sorghum, uncovering previously unrecognized diversity linked to key agronomic traits and environmental adaptation, a variation often missed when relying on a single reference genome [1,21,47,55].

A substantial fraction of TEs in the pangenome remained unclassified, likely reflecting lineage-specific or divergent TEs families underrepresented in existing repeat libraries [45,46]. These findings are consistent with recent large-scale pangenome efforts in sorghum, where more than 200 Mb of novel sequence were uncovered across cultivated and wild accessions [21,22,56]. Our analysis identified 28% of genes displaying PAVs, highlighting genomic diversity among elite lines. This proportion is comparable to elite maize accessions, where ~32% of gene transcripts in elite inbred lines display PAVs and are linked to stress- and environment-responsive functions as well as heterosis [57].

The PAVs suggest that multiple gene combinations may have been retained or selected to optimize adaptation and productivity across diverse growing environments. We discovered *SBE1* gene among pangenome-exclusive genes. In cereals like maize and rice, *SBE1* is associated with grain digestibility and quality, suggesting that its presence in elite U.S. sorghum likely reflects selection for processing traits and end-use preferences [58].

Despite the pangenome showing strong genome-wide collinearity and preserved telomere architecture, consistent with counter-selection against large-scale rearrangements [59], we identified a notable ~5 Mb inversion on chromosome 5 in ex-PVP lines. This region includes a WAK gene, part of a family known to regulate cell wall integrity and stress signaling in cold, drought, and salinity conditions [60,61] . In rice and Arabidopsis, WAK genes play central roles in early abiotic stress responses and cell wall remodeling, suggesting that this inversion may represent targeted selection for cold tolerance in temperate breeding programs.

Our genome-wide selective sweep analysis revealed strong signals of selection on circadian and photoperiodic regulators, extending beyond canonical domestication genes [31]. We detected a sweep at *SbPRR37 (Sobic.006G057866)*, the gene underlying the *Ma1* locus, a major repressor of flowering under long-day (LD) conditions. Recessive *ma1* alleles historically enabled early flowering and adaptation to temperate latitudes [62,63], while dominant *Ma1* alleles have been favored in modern biomass sorghum lines for delayed flowering under LD conditions by increasing expression of *SbCO* which repress *SbFT* thus extended vegetative growth [64,65]. Our observation of CNVs at *SbPRR37*—with two copies in most cultivated lines and one in wild haplotype 2—suggests differential selective pressure on photoperiod response across gene pools.

Additional sweeps at *PRR7, PRR95, Ma2, Ma6, VRN3b,* and *CO* underscore the polygenic nature of flowering-time control, integrating both classical *Ma* loci and newly implicated

regulators. Notably, genes such as *PHYA* exhibited copy number expansion in ex-PVP lines, which may enhance photoperiod sensitivity or stabilize developmental transitions under variable seasonal cues. The detection of enriched selection signals at *PHOT1, DET1,* and *XAP5* suggests that upstream regulatory pathways have been knowingly or unknowingly targeted during sorghum improvement. This highlights the importance of fine-tuned seasonal and environmental sensing in shaping phenological plasticity. Similar patterns have been observed in barley, where a natural variation at *Ppd-H1*, a *PRR7* ortholog, alters the circadian expression of flowering time genes without disrupting core clock components, enabling latitude-specific flowering responses [66]. In maize, selection on *ZmCCT9*, a diurnally regulated repressor of the florigen *ZCN8*, delays flowering under LD conditions and enhances adaptation to higher latitudes [67].

Beyond structural and genetic variation, we observed epigenomic divergence at functionally relevant loci, consistent with evidence that epigenetic modifications can be subject to selection and contribute to rapid adaptation, as demonstrated in *Arabidopsis thaliana* [68]. Notably, MATE transporter genes exhibited both a fourfold copy number expansion and reduced gene-body methylation in ex-PVP lines. These transporters mediate the efflux of organic acids, xenobiotics, and flavonoids, with established roles in herbicide detoxification and aluminum tolerance in cereals [69–72]. The observed gene-body hypomethylation may enhance expression under high-input agricultural conditions, suggesting that coordinated structural and epigenetic remodeling has been a feature of modern sorghum breeding.

Together, these results support a model in which sorghum's adaptation to temperate climates and agricultural intensification has been shaped by diverse molecular mechanisms—including targeted selection on flowering-time genes, clock genes, and epigenetic reprogramming of stress and detoxification genes. Our study complements and extends recent sorghum pangenome analyses [21,22,56,73], which established foundational catalogs of structural and gene-content diversity across races and wild sorghum relatives. While those efforts focused on broad germplasm panels, our study focuses on ex-PVP cultivars—historically important but under-characterized—and adds critical insights into how modern breeding has reshaped the genome.

Although this study offers major insights, limitations remain. The ex-PVP panel studied here represents lines from 1976–1992 and may not reflect recent commercial diversity. The functional impacts of structural variants and epialleles also require validation. Future work should integrate long-read resequencing, qPCR, and CRISPR to resolve complex loci. Additionally, field-based time-series transcriptomics are needed to link genomic variation with gene expression under natural conditions, improving our understanding of trait-environment interactions and guiding precision breeding.

In conclusion, this study demonstrates how modern breeding has shaped the sorghum genome through targeted structural, regulatory, and epigenetic changes, offering new opportunities for trait dissection and breeding innovation. The resulting pangenome resource enhances our ability to explore adaptation, gene-trait relationships, and the development of resilient, climate-smart sorghum varieties to meet global food, feed, and bioenergy demands.

469
470 **Methods**
471 **Plant Materials:** Seeds for 46 elite ex-Plant Variety Protection (ex-PVP) sorghum lines were
472 obtained from the USDA Germplasm Resources Information Network (GRIN). These
473 accessions originated from the breeding programs of Pioneer Hi-Bred International, Inc. (n =
474 39), Novartis Seeds, Inc. (n = 1), Cargill Wheat Research Farm (n = 1), Holden's Foundation
475 Seeds, Inc. (n = 1), Walter Moss Seed Company, LLC (n = 1), Ring Around Products, Inc. (n =
476 1), and Northrup, King & Company (n = 2). Wild sorghum accessions were also sourced from
477 GRIN and selected to represent diverse geographic and taxonomic origins for comparative
478 genomic analyses. RNA-seq was performed on two sorghum accessions, 'PI329478' and
479 'PI510757', using eight tissues per genotype: seedling, 3-leaf, 5-leaf, tiller, boot, panicle with
480 anthers, root, and dough-stage panicle. Total RNA was extracted, quality-checked, and used to
481 construct poly(A)-selected libraries, which were sequenced on an Illumina platform to produce
482 paired-end reads (Supplementary Table 12).
483 **High-Molecular-Weight (HMW) DNA Extraction and Sequencing:** HMW genomic DNA was
484 extracted from 3-week-old seedlings using Carlson lysis buffer and Qiagen Genomic-tips,
485 following the Oxford Nanopore Technologies (ONT) 'Plant leaf gDNA' protocol for Arabidopsis.
486 Samples were ground in liquid nitrogen, followed by two chloroform:isoamyl alcohol (24:1)
487 washes. Total Pure NGS beads (Omega Bio-tek) were used for cleanup. DNA was size-
488 selected for fragments >10–25 kb using the ONT Short Fragment Eliminator Kit (EXP-SFE001)
489 and quality assessed using the Agilent Genomic DNA ScreenTape system (5067-5365) or
490 Femto Pulse Genomic DNA 165 kb Kit (FP-1002-0275). HiFi circular consensus sequencing
491 (CCS) libraries were prepared using the PacBio protocol (PN 101-853-100 v5). Genomic DNA
492 was sheared using Covaris g-TUBEs to a modal fragment size of ~18 kb, and fragments <10 kb
493 were excluded using BluePippin S1 High Pass 6–10 kb cassettes.
494 **Genome Assembly and Annotation:** Ex-PVP genomes were assembled from Oxford
495 Nanopore Technologies (ONT) reads using Flye (v2.9.2), followed by polishing with Racon
496 (v1.5.0) and Pilon (v1.24) using Illumina short reads. Wild genomes were assembled using
497 Hifiasm (v0.16.1-r159) with PacBio HiFi reads. Assemblies were scaffolded using RagTag
498 (v2.1.0) with the BTx623 reference genome [16,74]. For the wild accession 'PI156549', Hi-C reads
499 were additionally aligned to contigs using the Juicer pipeline (v1.6.2), followed by scaffolding
500 with 3D-DNA (v180419). Manual curation was performed using Juicebox Assembly Tools
501 (v1.11.08). Genome assembly quality was evaluated using BUSCO (v5.4.3) with the
502 embryophyta_odb10 dataset and the LTR Assembly Index (LAI), which provides a metric for
503 assembly continuity and repeat completeness based on intact long terminal repeat
504 retrotransposons. Gene models were predicted using Helixer, a deep learning-based annotation
505 tool trained on plant genomes [44].
506 **Transposable Elements (TEs) Detection:** TEs were annotated using EDTA (v2.0.0) with the
507 flags --sensitive 1 and --anno 1, which integrates both structure- and homology-based
508 approaches. The pipeline incorporates multiple tools, including LTRharvest, LTR_FINDER,
509 LTR_retriever, Generic Repeat Finder, TIR-learner, HelitronScanner, TEsorter, RepeatModeler,
510 and RepeatMasker. Interspersed and tandem repeats were further annotated using
511 RepeatMasker (v4.1.1) with the custom EDTA-derived TE library, and tandem repeats were
512 identified with TRF (v4.09).

513
514 **Large Structural Variant Detection:** Structural variants (SVs) were identified using a
515 combination of reference-based and assembly-based approaches based on 46 exPVP and wild
516 accession PI156549. SYRI (https://github.com/schneebergerlab/syri) was first used to
517 characterize large-scale structural rearrangements, including translocations and inversions. For
518 assembly-based SV calling, Svim-asm (v1.0.3) was applied to genome assemblies to detect
519 insertions, deletions, and complex events. Additionally, CuteSV (v2.1.2) was used to extract
520 duplications (DUP), inversions (INV), and breakends (BND). SV results were refined and
521 benchmarked using Truvari (v5.3.0), and nonredundant SV sets were merged using SURVIVOR
522 (v1.0.7). Whole-genome alignments were performed using Minimap2 (v2.29-r1283) to support
523 SV analysis. Pangenome graph construction and structural diversity visualization were
524 performed using PGGB (v0.6.0).
525 **Synteny and Collinearity Analysis:** Conducted at both genome and gene levels using D-
526 Genies (v1.4) with whole-genome alignments from Minimap2 (v2.22), and MCScan in the JCVI
527 package (v1.2.7) based on CDS alignments of longest isoforms generated using Last (v1418).
528 **Identification of Orthologs:** The interspecific all orthogroup gene pairs were determined using
529 OrthoFinder (v2.5.4, ortho_opt: -M msa -A mafft -T fasttree)
530 **Single-Nucleotide Variant Calling, Admixture Analysis, and Population Structure**: Genome
531 assemblies from 46 ex-PVP lines and 25 wild sorghum accessions (Supplementary Table 1)
532 were aligned to the BTx623 v5 reference genome [16,75], and variants were called using
533 FreeBayes (v1.3.6) with a ploidy-aware setting (-g 1000). Variants were filtered to retain sites
534 with quality score (QUAL) > 30, yielding 494,424 SNPs and 33,132 INDELs (Source:
535 Fig4_Sbic2groups_wild_cultivated_variants.v1.freebayes.filt.vcf.gz). Filtered SNPs were further
536 refined and summarized using vcftools (v0.1.16) and rtg tools (v3.12) to retain only biallelic sites
537 with MAF between 0.01 and 0.99 and no more than 10% missing data, resulting in 34,035 high-
538 quality SNPs. These were used for population structure analysis. ADMIXTURE (v1.3.0) was run
539 with five-fold cross-validation for K = 1 to 10, identifying K = 2 as the optimal number of
540 ancestral populations based on the lowest CV error (Supplementary Fig. 2a-b). Population
541 structure was also assessed using principal component analysis (PCA) in PLINK (v1.90b7.7).
542 PCA separated accessions into three distinct clusters, with PC1 and PC2 explaining 30.34%
543 and 11.42% of the variation, respectively (Supplementary Fig. 2c-f).
544 **Selection Signature Identification:** We performed four pairwise comparisons using filtered
545 SNPs derived from whole-genome sequencing data: #1. Ex-PVP lines vs. all wild accessions.
546 #2. Ex-PVP lines vs. Wild1. #3. Ex-PVP lines vs. Wild2. #4. Wild1 vs. Wild2. For each
547 comparison, we employed three complementary methods to detect selective sweeps: FST
548 (fixation index):
549 Population differentiation was estimated using the Weir and Cockerham FST method
550 implemented in VCFtools. Analyses were performed using sliding windows of 100 kb with 10 kb
551 steps (--fst-window-size 100000 --fst-window-step 10000). Windows with FST > 0.3 were
552 considered indicative of strong differentiation. π-ratio (nucleotide diversity ratio): Nucleotide
553 diversity (π) was computed separately for each group using VCFtools (--window-pi 100000 --
554 window-pi-step 10000), and the ratio π exPVP / π wild was calculated. Windows with a π-ratio <
555 0.5 were interpreted as signals of reduced genetic diversity in the ex-PVP group, consistent with
556 selection. XP-CLR (Cross-Population Composite Likelihood Ratio): XP-CLR scores were

computed using XP-CLR (v1.1.2, https://github.com/hardingnj/xpclr), using a window size of 100 kb and step size of 10 kb. Windows in the top 1% (99th percentile) of XP-CLR scores were considered candidate regions under strong selection. We further defined high-confidence sweep regions using FST & XP-CLR intersection and FST & π-ratio & XP-CLR intersection. Only windows meeting all three thresholds were retained in the final sweep set, enhancing confidence that these represent genuine targets of selection during domestication or improvement.

DNA Methylation Analysis: LoReMe (Long Read Methylation) (Oxford Nanopore Technologies · GitHub) was used to infer DNA methylation patterns. In brief, the process involved the conversion of ONT FAST5 data to POD5 format using the Loreme Dorado-convert tool (v.0.3.1). Subsequently, super-high-accuracy base calling was performed, aligning the sequences to the reference genome. Modkit (v0.1.11) was employed to generate a bed file containing comprehensive methylation data, enabling us to create visual representations of methylation profiles for further investigation and interpretation.

Circadian Clock, Photoperiod, and Flowering Time Genes: Sorghum core circadian clock, light signaling, and flowering time orthologs genes were identified using known *Arabidopsis thaliana* genes as the seed [76]

Gene Ontology (GO) Enrichment Analysis: Genes located within or overlapping candidate sweep regions (±100 kb) were extracted by intersecting sweep windows with mRNA coordinates from the Sorghum bicolor BTx623 v5.1 reference annotation (Phytozome[16]). This was done using the PyRanges Python library. Genes from each metric-specific sweep set (e.g., FST-only, XP-CLR-only, triple-intersection) were analyzed separately. GO enrichment analysis was conducted using the GOATOOLS Python library (v1.2.3) with the find_enrichment.py script. GO term associations were generated from functional annotations predicted by eggNOG-mapper, and formatted into id2gos style association files. The GO DAG structure was derived from go-basic.obo. Each gene list was tested against a common background of all BTx623 genes with GO annotations. Statistically significant GO terms (corrected p-value < 0.05, using Benjamini-Hochberg FDR) were retained and reported.

Data Availability

All relevant datasets are provided in the main text and supplementary materials. Raw sequencing reads are publicly available under NCBI BioProject PRJNA1283509.
Analysis scripts and pipelines are available on GitHub at https://github.com/jkitony/Pangenome-of-U.S.-ex-PVP-and-Wild-Sorghum.
Genome assemblies and annotations can be accessed via the Salk Institute's resource portal (https://resources.michael.salk.edu/), Sorghumbase (https://www.sorghumbase.org/), and Figshare (https://doi.org/10.6084/m9.figshare.29261795.v4).

Acknowledgements

We would like to thank the Donald Danforth Plant Science Center, the United States Department of Agriculture (USDA), and the Germplasm Resources Information Network (GRIN) for providing resources used in this study. This work was supported through the Salk Harnessing Plants Initiative (HPI) with funding from the TED Audacious, Bezos Earth Fund, and Hess Corporation.

References

1. Paterson, A. H. *et al.* The Sorghum bicolor genome and the diversification of grasses. *Nature* **457**, 551–556 (2009).
2. Khoddami, A. *et al.* Sorghum in foods: Functionality and potential in innovative products. *Crit. Rev. Food Sci. Nutr.* (2023) doi:10.1080/10408398.2021.1960793.
3. George, T. T. *et al.* Trends and progress in sorghum research over two decades, and implications for global food security. *S. Afr. J. Bot.* **151**, 960–969 (2022).
4. House, L. R. A Guide to Sorghum Breeding Second Edition. 220 (1985).
5. Prasad, P. V. V., Staggenborg, S. A. & Ristic, Z. Impacts of drought and/or heat stress on physiological, developmental, growth, and yield processes of crop plants. in *Response of Crops to Limited Water* 301–355 (American Society of Agronomy and Soil Science Society of America, Madison, WI, USA, 2015).
6. Conner, A. B. *Hybrid Vigor in Sorghum*. (Texas Agricultural and Mechanical College System, 1927).
7. Reddy, P. S. & Reddy, B. V. S. History of sorghum improvement. in *Breeding Sorghum for Diverse End Uses* 61–75 (Elsevier, 2019).
8. Bird, J. A. The Northwestern Miller. *The Miller Publishing Company* **191**, (1937).
9. Wayne Smith, C. & Frederiksen, R. A. *Sorghum: Origin, History, Technology, and Production*. (John Wiley & Sons, 2000).
10. Klein, R. R. *et al.* The effect of tropical sorghum con version and inbred development on genome diversity as revealed by high-resolution genotyping. *Crop Sci* **48**, S12–S26 (2008).
11. Frederiksen, R. A. Proceedings of the Consultative Group Discussion on Research Needs and Strategies for Control of Sorghum Root and Stalk Rot Diseases. *International Crops Research Institute for the Semi-Arid Tropics* (1983).

627 12. Shahbandeh, M. Sorghum production by leading country worldwide 2023/24. *Statista*
628 (2024).
629 13. USDA. National Agricultural Statistics Service. *USDA* https://www.nass.usda.gov (2021).
630 14. Shakoor, N., Lee, S. & Mockler, T. C. High throughput phenotyping to accelerate crop
631 breeding and monitoring of diseases in the field. *Curr. Opin. Plant Biol.* **38**, 184–192 (2017).
632 15. McCormick, R. F. *et al.* The Sorghum bicolor reference genome: improved assembly, gene
633 annotations, a transcriptome atlas, and signatures of genome organization. *Plant J.* **93**,
634 338–354 (2018).
635 16. Morris, G. P. *et al.* Developing future resilience from signatures of adaptation across the
636 sorghum pangenome. *bioRxiv* 2025.08.01.667986 (2025).
637 17. Zhang, Z. *et al.* Major impacts of widespread structural variation on sorghum. *Genome Res.*
638 **34**, 286–299 (2024).
639 18. Lye, Z. N. & Purugganan, M. D. Copy number variation in domestication. *Trends Plant Sci.*
640 **24**, 352–365 (2019).
641 19. Zhang, D. *et al.* Chromosomal inversion at the DG1 promoter drives double-grain spikelets
642 and enhances grain yield in sorghum. *Nat. Plants* **11**, 453–467 (2025).
643 20. Lynch, R. C. *et al.* Domesticated cannabinoid synthases amid a wild mosaic cannabis
644 pangenome. *Nature* (2025) doi:10.1038/s41586-025-09065-0.
645 21. Tao, Y. *et al.* Extensive variation within the pan-genome of cultivated and wild sorghum.
646 *Nat. Plants* **7**, 766–773 (2021).
647 22. Ruperao, P. *et al.* Sorghum pan-genome explores the functional utility for genomic-assisted
648 breeding to accelerate the genetic gain. *Front. Plant Sci.* **12**, 666342 (2021).
649 23. Boatwright, J. L. *et al.* Sorghum Association Panel whole-genome sequencing establishes
650 cornerstone resource for dissecting genomic diversity. *Plant J.* **111**, 888–904 (2022).
651 24. Voelker, W. G. *et al.* Ten new high-quality genome assemblies for diverse bioenergy
652 sorghum genotypes. *bioRxiv* (2022) doi:10.1101/2022.09.26.509520.

653 25. Liu, F. *et al.* Unravelling sorghum functional genomics and molecular breeding: past
654 achievements and future prospects. *J. Genet. Genomics* (2024)
655 doi:10.1016/j.jgg.2024.07.016.
656 26. Deng, Y. *et al.* A complete assembly of the sorghum BTx623 reference genome. *Plant*
657 *Commun.* **5**, 100977 (2024).
658 27. Semagn, K. *et al.* Genetic diversity and selective sweeps in historical and modern
659 Canadian spring wheat cultivars using the 90K SNP array. *Sci. Rep.* **11**, 1–16 (2021).
660 28. Chen, S. *et al.* Genome-wide study of an elite rice pedigree reveals a complex history of
661 genetic architecture for breeding improvement. *Sci. Rep.* **7**, 1–12 (2017).
662 29. Yamasaki, M. *et al.* A Large-Scale Screen for Artificial Selection in Maize Identifies
663 Candidate Agronomic Loci for Domestication and Crop Improvement. *Plant Cell* **17**, 2859–
664 2872 (2005).
665 30. Han, Z. *et al.* Genomic signatures and candidate genes of lint yield and fibre quality
666 improvement in Upland cotton in Xinjiang. *Plant Biotechnol. J.* **18**, 2002–2014 (2020).
667 31. Lin, Z. *et al.* Parallel domestication of the Shattering1 genes in cereals. *Nat. Genet.* **44**,
668 720–724 (2012).
669 32. Li, X. & Yu, J. Unraveling the sorghum domestication. *Mol. Plant* **15**, 791–792 (2022).
670 33. Zhang, L.-M. *et al.* Sweet Sorghum Originated through Selection of Dry, a Plant-Specific
671 NAC Transcription Factor Gene. *Plant Cell* **30**, 2286–2307 (2018).
672 34. Creux, N. & Harmer, S. Circadian rhythms in plants. *Cold Spring Harb. Perspect. Biol.* **11**,
673 a034611 (2019).
674 35. Michael, T. P. Time of day analysis over a field grown developmental time course in rice.
675 *Plants* **12**, 166 (2022).
676 36. McClung, C. R. Circadian clock components offer targets for crop domestication and
677 improvement. *Genes (Basel)* **12**, 374 (2021).
678 37. Bendix, C., Marshall, C. M. & Harmon, F. G. Circadian clock genes universally control key

679 agricultural traits. *Mol. Plant* **8**, 1135–1152 (2015).
680 38. Yan, H. *et al.* The genetic diversity of 69 widely used Chinese sorghum hybrids released
681 between the 1970s and 2010s. *Agronomy (Basel)* **14**, 2180 (2024).
682 39. Maazou, A.-R. S. *et al.* Optimizing use of U.S. Ex-PVP inbred lines for enhancing
683 agronomic performance of tropical Striga resistant maize inbred lines. *BMC Plant Biol.* **22**,
684 286 (2022).
685 40. Hamblin, M. T. *et al.* Challenges of detecting directional selection after a bottleneck:
686 lessons from Sorghum bicolor. *Genetics* **173**, 953–964 (2006).
687 41. Jordan, D. R., Mace, E. S., Cruickshank, A. W., Hunt, C. H. & Henzell, R. G. Exploring and
688 exploiting genetic variation from unadapted sorghum germplasm in a breeding program.
689 *Crop Sci.* **51**, 1444–1457 (2011).
690 42. Coffman, S. M., Hufford, M. B., Andorf, C. M. & Lübberstedt, T. Haplotype structure in
691 commercial maize breeding programs in relation to key founder lines. *Theor. Appl. Genet.*
692 **133**, 547–561 (2020).
693 43. Deneweth, J., Van de Peer, Y. & Vermeirssen, V. Nearby transposable elements impact
694 plant stress gene regulatory networks: a meta-analysis in A. thaliana and S. lycopersicum.
695 *BMC Genomics* **23**, 18 (2022).
696 44. Stiehler, F. *et al.* Helixer: cross-species gene annotation of large eukaryotic genomes using
697 deep learning. *Bioinformatics* **36**, 5291–5298 (2021).
698 45. Ou, S. *et al.* Benchmarking transposable element annotation methods for creation of a
699 streamlined, comprehensive pipeline. *Genome Biol.* **20**, 275 (2019).
700 46. Wicker, T. *et al.* A unified classification system for eukaryotic transposable elements. *Nat.*
701 *Rev. Genet.* **8**, 973–982 (2007).
702 47. Zhao, K. *et al.* Pangenome analysis reveals structural variation associated with seed size
703 and weight traits in peanut. *Nat. Genet.* 1–12 (2025).
704 48. Biswas, S. *et al.* Increasing the level of resistant starch in ‘Presidio’ rice through multiplex

705 CRISPR-Cas9 gene editing of starch branching enzyme genes. *Plant Genome* **16**, e20225
706 (2023).
707 49. Zhou, Z. *et al.* Resequencing 302 wild and cultivated accessions identifies genes related to
708 domestication and improvement in soybean. *Nat. Biotechnol.* **33**, 408–414 (2015).
709 50. Della Coletta, R., Qiu, Y., Ou, S., Hufford, M. B. & Hirsch, C. N. How the pan-genome is
710 changing crop genomics and improvement. *Genome Biol.* **22**, 3 (2021).
711 51. Liao, Z. *et al.* Structural variations in papaya genomes. *BMC Genomics* **22**, 335 (2021).
712 52. Zhang, H., Kumimoto, R. W., Anver, S. & Harmer, S. L. XAP5 CIRCADIAN TIMEKEEPER
713 regulates RNA splicing and the circadian clock by genetically separable pathways. *Plant*
714 *Physiol.* **192**, 2492–2506 (2023).
715 53. Prusty, M. R. *et al.* Genetic loci mediating circadian clock output plasticity and crop
716 productivity under barley domestication. *New Phytol.* **230**, 1787–1801 (2021).
717 54. Ku, Y.-S., Cheng, S.-S., Cheung, M.-Y. & Lam, H.-M. The roles of multidrug and toxic
718 compound extrusion (MATE) transporters in regulating agronomic traits. *Agronomy (Basel)*
719 **12**, 878 (2022).
720 55. Mace, E. S. *et al.* Whole-genome sequencing reveals untapped genetic potential in Africa's
721 indigenous cereal crop sorghum. *Nat. Commun.* **4**, 2320 (2013).
722 56. Marla, S. R. *et al.* Mining sorghum pangenome enabled identification of new dw3 alleles for
723 breeding stable-dwarfing hybrids. *G3 (Bethesda)* **15**, (2025).
724 57. Hirsch, C. N. *et al.* Draft assembly of elite inbred line PH207 provides insights into genomic
725 and transcriptome diversity in maize. *Plant Cell* **28**, 2700–2714 (2016).
726 58. Xia, H., Yandeau-Nelson, M., Thompson, D. B. & Guiltinan, M. J. Deficiency of maize
727 starch-branching enzyme I results in altered starch fine structure, decreased digestibility
728 and reduced coleoptile growth during germination. *BMC Plant Biol.* **11**, 95 (2011).
729 59. Lian, Q. *et al.* A pan-genome of 69 Arabidopsis thaliana accessions reveals a conserved
730 genome structure throughout the global species range. *Nat. Genet.* **56**, 982–991 (2024).

731 60. Kohorn, B. D. & Kohorn, S. L. The cell wall-associated kinases, WAKs, as pectin receptors.
732 *Front. Plant Sci.* **3**, 88 (2012).
733 61. Wu, Q. *et al.* CsWAK12, a novel cell wall-associated receptor kinase gene from Camellia
734 sinensis, promotes growth but reduces cold tolerance in Arabidopsis. *Front. Plant Sci.* **15**,
735 1420431 (2024).
736 62. Quinby, J. R. Fourth maturity gene locus in sorghum 1. *Crop Sci.* **6**, 516–518 (1966).
737 63. Quinby, J. R. The genetics of sorghum improvement. *J. Hered.* **66**, 56–62 (1975).
738 64. Murphy, R. L. *et al.* Coincident light and clock regulation of pseudoresponse regulator
739 protein 37 (PRR37) controls photoperiodic flowering in sorghum. *Proc. Natl. Acad. Sci. U.*
740 *S. A.* **108**, 16469–16474 (2011).
741 65. Mullet, J. *et al.* Energy sorghum--a genetic model for the design of C4 grass bioenergy
742 crops. *J. Exp. Bot.* **65**, 3479–3489 (2014).
743 66. Campoli, C., Shtaya, M., Davis, S. J. & von Korff, M. Expression conservation within the
744 circadian clock of a monocot: natural variation at barley Ppd-H1 affects circadian
745 expression of flowering time genes, but not clock orthologs. *BMC Plant Biol.* **12**, 97 (2012).
746 67. Huang, C. *et al.* ZmCCT9 enhances maize adaptation to higher latitudes. *Proc. Natl. Acad.*
747 *Sci. U. S. A.* **115**, E334–E341 (2018).
748 68. Schmid, M. W. *et al.* Contribution of epigenetic variation to adaptation in Arabidopsis. *Nat.*
749 *Commun.* **9**, 4446 (2018).
750 69. Maron, L. G. *et al.* Aluminum tolerance in maize is associated with higher*MATE1*gene copy
751 number. *Proc. Natl. Acad. Sci. U. S. A.* **110**, 5241–5246 (2013).
752 70. Magalhaes, J. V. *et al.* A gene in the multidrug and toxic compound extrusion (MATE)
753 family confers aluminum tolerance in sorghum. *Nat. Genet.* **39**, 1156–1161 (2007).
754 71. Du, Z. *et al.* Genome-wide characterization of MATE gene family and expression profiles in
755 response to abiotic stresses in rice (Oryza sativa). *BMC Ecol. Evol.* **21**, 141 (2021).
756 72. Zhou, G., Delhaize, E., Zhou, M. & Ryan, P. R. The barley MATE gene, HvAACT1,

757 increases citrate efflux and Al(3+) tolerance when expressed in wheat and barley. *Ann. Bot.*
758 **112**, 603–612 (2013).
759 73. Chen, C. *et al.* A comprehensive omics resource and genetic tools for functional genomics
760 research and genetic improvement of sorghum. *Mol. Plant* **18**, 703–719 (2025).
761 74. Alonge, M. *et al.* RaGOO: fast and accurate reference-guided scaffolding of draft genomes.
762 *Genome Biol.* **20**, 224 (2019).
763 75. Gladman, N. *et al.* SorghumBase: a web-based portal for sorghum genetic information and
764 community advancement. *Planta* **255**, 35 (2022).
765 76. Michael, T. P. Core circadian clock and light signaling genes brought into genetic linkage
766 across the green lineage. *Plant Physiol.* **190**, 1037–1056 (2022).

767